Light Diffraction by a Strong Standing Electromagnetic Wave

A. Di Piazza,[*] K. Z. Hatsagortsyan,[†] and C. H. Keitel[‡]

Max-Planck-Institut für Kernphysik, Saupfercheckweg 1, D-69117 Heidelberg, Germany
(Received 3 February 2006; published 24 August 2006)

The nonlinear quantum interaction of a linearly polarized x-ray probe beam with a focused intense standing laser wave is studied theoretically. Because of the tight focusing of the standing laser pulse, diffraction effects arise for the probe beam as opposed to the corresponding plane wave scenario. A quantitative estimate for realistic experimental conditions of the ellipticity and the rotation of the main polarization plane acquired by the x-ray probe after the interaction shows that the implementation of such vacuum effects is feasible with future X-ray Free Electron Laser light.

Since the early work by Heisenberg and Euler [1], the electromagnetic properties of vacuum are known in principle to be modified by the presence of strong electromagnetic fields [2]. The associated scales for the electric and magnetic field amplitudes are governed by the so-called critical electric $E_{cr} = m^2c^3/\hbar e = 1.3 \times 10^{16}$ V/cm and magnetic $B_{cr} = m^2c^3/\hbar e = 4.4 \times 10^{13}$ G fields with negative electron charge $-e$ and electron mass m. In the presence of such strong fields, vacuum generally behaves as a nonlinear, birefringent, and dichroic dielectric medium. In particular, the vacuum polarization has been studied in the presence of static and uniform electromagnetic fields in various configurations [3]. Given the extremely large values of E_{cr} and B_{cr} it remains very challenging though to experimentally verify vacuum nonlinearities by means of static and uniform fields. The PVLAS (Polarizzazione del Vuoto con Laser) experiment has recently been designed to measure the extremely small ellipticity acquired by a linearly polarized probe laser after passing repeatedly through a vacuum region with applied static uniform magnetic field of strength 5.5×10^4 G [4]. We note that most recently first experimental results from the PVLAS project on the rotation of light polarization in vacuum have been reported in [5]. Nevertheless, those results cannot be explained as a nonlinear quantum electrodynamics (QED) effect but as a dichroic effect due to the possible conversion of a photon into a pseudoscalar particle, called axion.

Much stronger electromagnetic fields can be produced by means of focused laser pulses. Laser intensities up to 10^{21}–10^{22} W/cm^2 have already been obtained in the so-called λ^3 regime [6]. Envisaged intensities of order 10^{24}–10^{26} W/cm^2 corresponding to peak electric fields 10^{13}–10^{14} V/cm are likely to be reached in the near future [7]. At present, elastic light-light interaction has not been experimentally revealed via strong laser pulses (see also [8]). On the theoretical side, photon propagation was evaluated to be modified in the presence of an intense plane wave [9,10]. Recently, the analogous problem of the propagation of an x-ray photon along a standing wave has been considered in [11] by estimating the effects of the laser

pulse profile along the propagation direction. With the recent development of extremely focused laser beams, a theoretical treatment becomes necessary though which fully takes into account of the three-dimensional spatial confinement of the fields.

In the present Letter we investigate how extreme spatial confinement of crossed laser fields gives rise to diffraction effects in the interaction between probe and intense laser beams. The virtues of a high-frequency probe field with good spatial coherence and a large photon number per pulse become apparent such that the envisaged X-ray Free Electron Laser (X-FEL) at Deutsches Elektronen-Synchrotron in Hamburg appears suitable. The required focusing of the laser pulses turns out to yield a significant reduction of the observable vacuum nonlinearities while experimental verification is shown to be feasible for realistic near future parameters.

Since vacuum polarization effects are larger with shorter probe wavelength, we study the interaction of an *x-ray* probe beam by a standing wave generated by the superposition of two counterpropagating strong and tightly focused optical laser beams. The advantage of a standing wave instead of a single laser wave is a larger coupling strength in the configuration in which the probe wave propagates perpendicularly to the strong beam. Our configuration also turns out to be more favorable because the deteriorating role of diffraction on vacuum effects is reduced.

In the present experimental conditions it is appropriate to assume that the amplitude and the frequency of both the probe and the strong field are much less than E_{cr} and m, respectively (from now on natural units with $\hbar = c = 1$ are used). Further, we have ensured that here the axion effect is completely negligible, essentially due to the microscopic dimensions of the interaction region of the two beams (see also [12]). For these reasons our starting point is the Euler-Heisenberg Lagrangian density at lowest order [2]:

$$\mathcal{L} = \frac{1}{2}(E^2 - B^2) + \frac{2\alpha^2}{45m^4}[(E^2 - B^2)^2 + 7(\mathbf{E} \cdot \mathbf{B})^2], \quad (1)$$

with fine-structure constant $\alpha = e^2/4\pi$ and total electric and magnetic field $\mathbf{E}(\mathbf{r}, t)$ and $\mathbf{B}(\mathbf{r}, t)$, respectively. The

second term in the previous Lagrangian density can be considered as a small perturbation of the Maxwell Lagrangian density $(E^2 - B^2)/2$. The Lagrangian density in Eq. (1) yields the following nonlinear wave equation for the electric field:

$$\nabla^2 \mathbf{E} - \partial_t^2 \mathbf{E} = \mathcal{J}(\mathbf{r}, t), \qquad (2)$$

where

$$\mathcal{J}(\mathbf{r}, t) = \nabla \times (\partial_t \mathbf{M}) + \partial_t^2 \mathbf{P} - \nabla(\nabla \cdot \mathbf{P}) \qquad (3)$$

with polarization $\mathbf{P}(\mathbf{r}, t) = 4\alpha^2/(45m^4)[2(E^2 - B^2)\mathbf{E} + 7(\mathbf{E} \cdot \mathbf{B})\mathbf{B}]$ and magnetization $\mathbf{M}(\mathbf{r}, t) = 4\alpha^2/(45m^4) \times [2(E^2 - B^2)\mathbf{B} - 7(\mathbf{E} \cdot \mathbf{B})\mathbf{E}]$. Since the quantity $\mathcal{J}(\mathbf{r}, t)$ is very small, this nonlinearity of the wave equation (2) can be accounted for by a perturbative approach. Up to first order, the solution of Eq. (2) can be expressed as $\mathbf{E}(\mathbf{r}, t) \approx \mathbf{E}^{(0)}(\mathbf{r}, t) + \mathbf{E}_{\text{diff}}(\mathbf{r}, t)$, where $\mathbf{E}^{(0)}(\mathbf{r}, t) = \mathbf{E}_0(\mathbf{r}, t) + \mathbf{E}_p(\mathbf{r}, t)$ is the zero-order solution with $\mathbf{E}_0(\mathbf{r}, t)$ being the strong standing wave electric field and $\mathbf{E}_p(\mathbf{r}, t)$ the probe electric field and where

$$\mathbf{E}_{\text{diff}}(\mathbf{r}, t) = -\frac{1}{4\pi} \int_V d\mathbf{r}' \frac{\mathcal{J}^{(1)}(\mathbf{r}', t - |\mathbf{r} - \mathbf{r}'|)}{|\mathbf{r} - \mathbf{r}'|} \qquad (4)$$

is the diffracted wave generated by the nonlinear QED interaction of the probe with the strong standing wave. This interaction breaks the space isotropy [see Eq. (1)], and the symmetry breaking manifests itself in the field correction $\mathbf{E}_{\text{diff}}(\mathbf{r}, t)$. In Eq. (4) it is understood that the point $\mathbf{r}$ lies outside the interaction volume V defined by the condition $\mathcal{J}^{(1)}(\mathbf{r}, t) \neq \mathbf{0}$. $\mathcal{J}^{(1)}(\mathbf{r}, t)$ is obtained by substituting the fields in Eq. (3) by their corresponding zero-order expressions $\mathbf{E}^{(0)}(\mathbf{r}, t)$ and $\mathbf{B}^{(0)}(\mathbf{r}, t)$. Further, we assume that the strong standing wave results from the superposition of two Gaussian beams propagating along the z axis in opposite directions and both with polarization along the x axis, amplitude $E_0/\sqrt{2}$, frequency ω_0, and waist size w_0 (see Fig. 1) [13], yielding

$$\mathbf{E}_0(\mathbf{r}, t) = \sqrt{2} E_0 \frac{e^{-(x^2+y^2)/w^2(z)}}{\sqrt{1 + (z/z_r)^2}} \sin(\psi_0 + \omega_0 t)$$
$$\times \cos\left(k_0 z - \tan^{-1}\frac{z}{z_r} + \frac{k_0 z}{2}\frac{x^2 + y^2}{z^2 + z_r^2}\right) \hat{\mathbf{x}}, \qquad (5)$$

with $k_0 = \omega_0$, $w(z) = w_0\sqrt{1 + (z/z_r)^2}$, and Rayleigh length $z_r = k_0 w_0^2/2$. The factor $1/\sqrt{2}$ in the amplitude of the superimposed beams has been inserted to take into account that usually in experiments the standing wave is obtained by first splitting the beam of one laser field. In general, Eq. (5) is nearly an approximate solution of Maxwell's equations when $w_0/z_r \ll 1$. We have shown that our final results are valid up to terms proportional to $(w_0/z_r)^2$, which is much smaller than 1 even in the case of a maximally focused beam with $w_0 = \lambda_0 = 2\pi/k_0$. As opposed to the strong standing wave, the probe beam usually is neither tightly focused nor very strong. For these
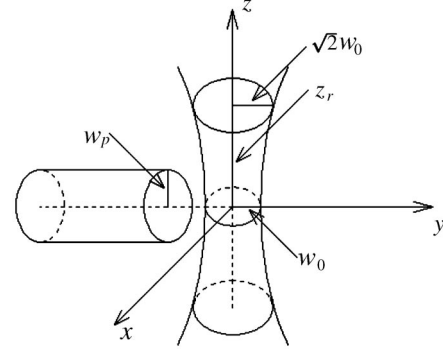

FIG. 1. Geometry depicting the interaction of the two beams. All symbols are described between Eqs. (4) and (7).

reasons, if we assume that the probe field propagates along the y axis and that it is polarized in the x-z plane, we can write the probe electric field as

$$\mathbf{E}_p(\mathbf{r}, t) = E_p e^{-(x^2+z^2)/w_p^2} \sin(\psi_p + \omega_p t - k_p y)$$
$$\times (\hat{\mathbf{z}} \sin\vartheta + \hat{\mathbf{x}} \cos\vartheta) \qquad (6)$$

with probe frequency $\omega_p = k_p$ and probe waist size w_p (see Fig. 1). In Fourier space Eq. (4) becomes

$$\mathbf{E}_{\text{diff}}(\mathbf{r}, \omega) = -\frac{1}{4\pi} \int_V d\mathbf{r}' \frac{e^{i\omega|\mathbf{r}-\mathbf{r}'|}}{|\mathbf{r} - \mathbf{r}'|} \mathcal{J}^{(1)}(\mathbf{r}', \omega). \qquad (7)$$

We are interested in the effects of the strong standing wave on the probe field. Then we fix $\omega = \omega_p$ and the detection point $\mathbf{r}$ along the probe field propagation axis, i.e., $\mathbf{r} = \mathbf{r}_d \equiv (0, y_d, 0)$ with $y_d > w_0$ (see Fig. 1). Moreover, to analyze the diffracted field evolution along its propagation to $\mathbf{r}_d$, we write a general expression for the diffracted field which is valid in the near as well as in the far zone as defined below. This can be realized by adopting the following conditions: on one hand, $y_d \gg w_p, w_0, z_r$, and on the other hand, $(w_0/\lambda_p)(w_p/y_d)^2 \ll 1$ and $(w_p/\lambda_p) \times (w_p/y_d)^3 \ll 1$, with probe wavelength $\lambda_p = 2\pi/\omega_p$. From an experimental point of view, the previous conditions are not very restrictive. For example, if $w_0 \sim \lambda_0 \lesssim 1$ μm, $y_d \gtrsim 1$ cm, and $\lambda_p \gtrsim 10^{-3}$ μm, these inequalities are fulfilled if $w_p \lesssim 100$ μm. Now, if we set

$$\mathbf{E}_{\text{diff}}(\mathbf{r}_d, t) = -\mathbf{E}_{\text{diff}}(\mathbf{r}_d)\frac{e^{-i(\psi_p + \omega_p t - k_p y_d)}}{2i} + \text{c.c.}, \qquad (8)$$

we obtain for the above parameter region

$$\mathbf{E}_{\text{diff}}(\mathbf{r}_d) = \frac{\omega_p^2}{4\pi}\frac{E_p}{2}(7\sin\vartheta\hat{\mathbf{z}} + 4\cos\vartheta\hat{\mathbf{x}})\frac{\alpha}{45\pi}\left(\frac{E_0}{E_{cr}}\right)^2 \frac{\mathcal{V}}{y_d}, \qquad (9)$$

where the complex integration

$$\mathcal{V} = \int_V d\mathbf{r}' e^{-(1/w_p^2 - i\omega_p/2y_d)(x'^2+z'^2)} \frac{e^{-2(x'^2+y'^2)/w^2(z')}}{1 + (z'/z_r)^2}$$
$$\times \left[1 + \cos 2\left(k_0 z' - \tan^{-1}\frac{z'}{z_r} + \frac{k_0 z'}{2}\frac{x'^2 + y'^2}{z'^2 + z_r^2}\right)\right] \qquad (10)$$

should be performed over the finite volume V of the interaction region. Furthermore, the three-dimensional integral over $\mathbf{r}'$ is rapidly convergent in the limit $V \to \infty$ so that we can evaluate it in this limit with no appreciable error. Hence, with $w_p/\lambda_0 \gg \sqrt[4]{1 + (\pi w_p^2/y_d\lambda_p)^2}$, the cos term in the integrand yields a negligible contribution with respect to the remaining integration that can be performed exactly. For example, if $\lambda_0 \lesssim 1\ \mu\text{m}$, $w_p \gtrsim 8\ \mu\text{m}$, and $\lambda_p \gtrsim 10^{-3}\ \mu\text{m}$, this approximation applies well in the region $y_d \gtrsim 2$ cm. Then we obtain

$$\mathcal{V} = \frac{\pi}{\sqrt{2}} \frac{w_0 w_p z_r}{\sqrt{1 - i\pi \frac{w_p^2}{y_d\lambda_p}}} \exp\left[z_r^2 \left(\frac{1}{2}\frac{1}{w_p^2} + \frac{1}{w_0^2} - i\frac{\pi}{2}\frac{1}{y_d\lambda_p} \right) \right]$$

$$\times K_0\left[z_r^2 \left(\frac{1}{2}\frac{1}{w_p^2} + \frac{1}{w_0^2} - i\frac{\pi}{2}\frac{1}{y_d\lambda_p} \right) \right] \quad (11)$$

with $K_0(z)$ being the zero-order modified Bessel function [14]. By adding the diffracted field to the probe field in Eq. (6) we obtain that the resulting field is elliptically polarized in the x-z plane and that the major axis of the ellipse is rotated with respect to the initial probe polarization direction. The two relevant parameters, i.e., the rotation angle of the major axis of the ellipse and the ellipticity, are given, respectively, by

$$\psi = \frac{\omega_p}{8\pi} \frac{3\alpha}{45\pi} \frac{I_0}{I_{\text{cr}}} \frac{\omega_p \mathcal{V}_r}{2y_d} \sin 2\vartheta, \quad (12)$$

$$\varepsilon = \frac{\omega_p}{8\pi} \frac{3\alpha}{45\pi} \frac{I_0}{I_{cr}} \frac{\omega_p \mathcal{V}_i}{2y_d} \sin 2\vartheta \quad (13)$$

with the real (imaginary) part $\mathcal{V}_r$ ($\mathcal{V}_i$) of $\mathcal{V}$, strong laser intensity I_0, and $I_{\text{cr}} = E_{\text{cr}}^2/8\pi = 2.3 \times 10^{29}\ \text{W/cm}^2$. Since the diffracted field $\mathbf{E}_{\text{diff}}(\mathbf{r}, t)$ is generated by a localized source inside V, it is not a plane wave and its amplitude depends on the observation distance y_d as do ψ and ε.

Equations (12) and (13) and the analytical expression (11) allow one to analyze the evolution along the propagation direction of the polarization of the probe field after the diffraction by the strong standing wave. The typical length of the interaction region is w_0 in the x direction and w_p in the z direction and they determine the diffraction parameters: $\xi_0 = w_0^2/y_d\lambda_p$ and $\xi_p = w_p^2/y_d\lambda_p$. In turn, these determine the field zones: the "near zone," if $\xi_0, \xi_p \gg 1$, where the diffraction effects along both the x and the z axis are negligible; the "far zone," if $\xi_0, \xi_p \ll 1$, where the diffraction effects are very important.

Only in the near zone does one obtain results analogous to those in [9,11] because the spatial confinement of the fields transverse to the probe propagation direction does not play any role. In this zone, on one hand, the rotation angle ψ is much smaller than the ellipticity being the dominating imaginary part of $\mathcal{V} \approx i\sqrt{2\pi^3} w_0 y_d/\omega_p$ in Eq. (11). On the other hand, the ellipticity does not depend on the observation distance and it can be written as $2\varepsilon = \omega_p l(n_\perp - n_\parallel)\sin 2\vartheta$. In this expression l is the distance covered by the probe in the presence of the strong field and $n_{\parallel,\perp}$ are two different vacuum refractive indices depending on the mutual orientation of the probe and the strong field polarization directions. In our case $l = 2w_0$ and $n_{\parallel,\perp} = 1 + \sqrt{\pi/2}c_{\parallel,\perp}\alpha/(360\pi)I_0/I_{\text{cr}}$ with $c_\parallel = 4$ and $c_\perp = 7$. However, we stress that the near zone is hardly realizable experimentally. For example, if $w_0 \lesssim 1\ \mu\text{m}$, the condition $\xi_0 \gg 1$ requires observation distances $y_d \ll 1$ cm even in the case of x-ray probes.

In the far zone where $\xi_0, \xi_p \ll 1$, $\mathcal{V}$ is independent of y_d and becomes real. Then the polarization of the probe field remains linear but its polarization direction is rotated appreciably by ψ. In particular, if $w_p \gg w_0$, then $\mathcal{V} \approx \pi^{3/2}w_p w_0^2/2$. Therefore, the polarization rotation angle ψ in the far zone is $\pi\sqrt{\xi_p\xi_0/2}$ times smaller than the ellipticity in the near zone. However, we note that at observation distances with $\xi_p < 1/\pi$ the defocusing of the probe field is no longer negligible. For a precise rather than above order-of-magnitude estimate, correcting terms proportional to $1/(\pi\xi_p)$ should be included in Eq. (6).

In the remaining intermediate zone the most general situation happens in which the polarization rotation angle ψ and the ellipticity ε alter similarly. In Fig. 2 we plot ψ and ε as functions of the observation distance y_d and find detectable values. In the numerical estimates we have used the exact expression (10) of $\mathcal{V}$ and ensured that the analytic expression (11) reproduces the numerical values up to 0.1%. In order to maximize the vacuum effects, we set $\vartheta = \pi/4$. Concerning the strong field we employ the feasible intensity $I_0 = 10^{23}\ \text{W/cm}^2$ and $w_0 = \lambda_0 = 0.745\ \mu\text{m}$. With respect to the probe field we set $\lambda_p = 0.4$ nm and $w_p = 8\ \mu\text{m}$. Note that in Fig. 2 we avoided both the far zone as mentioned above and the near zone because already at the quite small observation distance $y_d = 2$ cm we merely achieve $\xi_0 = 0.07$. Nevertheless, Fig. 2 confirms that at small y_d the ellipticity is larger than the polarization rotation angle and vice versa for large
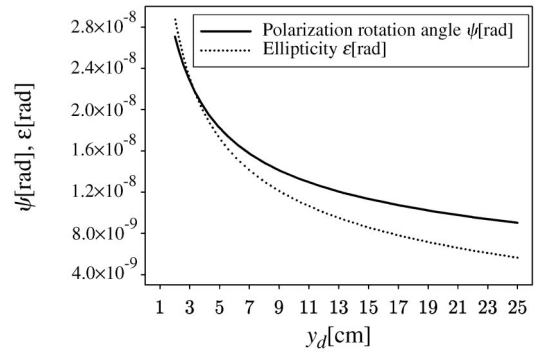

FIG. 2.   The polarization rotation angle ψ and the ellipticity ε as functions of the observation distance y_d. We set $\vartheta = \pi/4$, $w_0 = \lambda_0 = 0.745\ \mu\text{m}$, $I_0 = 10^{23}\ \text{W/cm}^2$, $w_p = 8\ \mu\text{m}$, and $\lambda_p = 0.4$ nm, yielding $\xi_0 = 0.14/(y_d[\text{cm}])$ and $\xi_p = 16/(y_d[\text{cm}])$.

y_d. In general, as expected, the vacuum effects are larger at small y_d when the effects of the diffraction along z become smaller. This reduction is intuitively clear because diffraction induces a spreading and consequently an attenuation of the generated field. Furthermore, diffraction effects along x can hardly be avoided. In this respect, the head-on collision of a probe field with a single laser pulse is less favorable than our crossed beam scenario because the diffraction effects then cannot be neglected along both axes x and z.

In the plane wave approximation one neglects both the diffraction effects and the spatial confinement of the probe and the strong beams. In this case we note that the value of the ellipticity acquired by a probe with wavelength $\lambda_p = 0.4$ nm after crossing a region with $2w_0 = 1.5$ μm and standing wave intensity $I_0 = 10^{23}$ W/cm^2 is 4×10^{-7} rad, i.e., more than 1 order of magnitude larger than our results including spatial confinement and diffraction. Nevertheless, Fig. 2 also shows that with the above parameters and despite diffraction, the polarization rotation angle and the ellipticity are still more than 2 orders of magnitude larger than the estimated ellipticity induced by nonlinear QED effects in the PVLAS setup with $\varepsilon_{PVLAS} = 5 \times 10^{-11}$ rad [4]. We stress also that our method is single passage, which does not require an optical cavity as in the PVLAS experiment.

The presence of charged particles in the interaction region may conceal vacuum effects. The maximum pressure P_M of an electron gas in the interaction region to render the effects of Thompson scattering of the probe field negligible can be estimated as $P_M \sim 10^{-6}$ torr for the parameters in Fig. 2 and temperature $T = 300$ K. Such a high-quality vacuum are obtained nowadays (see, e.g., [5]).

Another question is if today's x-ray polarimeters can measure small ellipticities and/or polarization rotation angles as obtained above. By exploiting multiple Bragg reflections by channel-cut crystals, polarimeter sensitivities of order 10^{-6}–10^{-5} rad can be reached in principle [15]. Since $\psi, \varepsilon \propto I_0$ [see Eq. (13)], to obtain such values, strong field intensities of order 10^{25}–10^{26} W/cm^2 are required which are quite feasible in the near future [7]. Furthermore, at photon wavelengths $\lambda_p = 0.4$ nm typical values of the modulation factor and of the efficiency of an x-ray detector are around $20\% - 30\%$ [16]. Then, in order to measure, for example, polarization rotation angles $\psi \sim 10^{-5}$ rad, the probe beam should provide for each pulse at least of order 10^{12}–10^{13} photons. Moreover, due to the small angular acceptance of the channel-cut crystals $\Delta\theta \sim 1$ μrad, a highly collimated x-ray probe with beam divergence up to $\Delta\theta$ is required in order to reach the mentioned values of sensitivities. Then, the probing of vacuum nonlinearities can represent a further challenging application for the future X-FEL because it is likely to fulfill both previous conditions on the number of photons per pulse and on the beam divergence [17]. Finally, the initial polar-

ization degree of the X-FEL has to be sufficiently high to allow for the measurement of polarization rotation angles ψ of order of 10^{-5} rad. If this is not the case, the X-FEL beam needs to be further polarized by employing, for example, the technique described in [15].

In conclusion, we have shown that diffraction and spatial confinement of the fields are essential in describing the interaction between a strong tightly focused optical standing wave and an x-ray probe beam. The ellipticity and the polarization rotation angle acquired by the probe after the interaction with the strong field were evaluated analytically. We have demonstrated that while these variables are considerably smaller than those estimated in the usually considered plane wave approximation, they should be measurable in the near future.

*Electronic address: dipiazza@mpi-hd.mpg.de
†Electronic address: k.hatsagortsyan@mpi-hd.mpg.de
‡Electronic address: keitel@mpi-hd.mpg.de

[1] W. Heisenberg and H. Euler, Z. Phys. **98**, 714 (1936).

[2] W. Dittrich and H. Gies, *Probing the Quantum Vacuum* (Springer-Verlag, Berlin, 2000), Chap. 2.

[3] J. J. Klein and B. P. Nigam, Phys. Rev. **135**, B1279 (1964); N. B. Narozhnyĭ, Sov. Phys. JETP **28**, 371 (1969); Z. Bialynicka-Birula and I. Bialynicki-Birula, Phys. Rev. D **2**, 2341 (1970); E. Brezin and C. Itzykson, Phys. Rev. D **3**, 618 (1971); I. A. Batalin and A. E. Shabad, Sov. Phys. JETP **33**, 483 (1971); V. I. Ritus, Ann. Phys. (N.Y.) **69**, 555 (1972); J. K. Daugherty and I. Lerche, Phys. Rev. D **14**, 340 (1976); L. F. Urrutia, Phys. Rev. D **17**, 1977 (1978).

[4] D. Bakalov *et al.*, Quantum Semiclass. Opt. **10**, 239 (1998).

[5] E. Zavattini *et al.*, Phys. Rev. Lett. **96**, 110406 (2006).

[6] S.-W. Bahk *et al.*, Opt. Lett. **29**, 2837 (2004).

[7] T. Tajima and G. Mourou, Phys. Rev. ST Accel. Beams **5**, 031301 (2002).

[8] E. Lundström *et al.*, Phys. Rev. Lett. **96**, 083602 (2006).

[9] W. Becker and H. Mitter, J. Phys. A **8**, 1638 (1975); V. N. Baier, A. I. Mil'shtein, and V. M. Strakhovenko, Sov. Phys. JETP **42**, 961 (1976); I. Affleck, J. Phys. A **21**, 693 (1988).

[10] E. B. Aleksandrov, A. A. Ansel'm, and A. N. Moskalev, Sov. Phys. JETP **62**, 680 (1986).

[11] T. Heinzl *et al.*, hep-ph/0601076.

[12] G. Raffelt and L. Stodolsky, Phys. Rev. D **37**, 1237 (1988).

[13] Y. I. Salamin and C. H. Keitel, Phys. Rev. Lett. **88**, 095005 (2002).

[14] I. M. Ryzhik and I. S. Gradshteyn, *Tables of Integrals, Series and Products* (Academic Press, London, 1965).

[15] E. E. Alp, W. Sturhahn, and T. S. Toellner, Hyperfine Interact. **125**, 45 (2000).

[16] P. Soffitta (private communication); see also P. Soffitta *et al.*, Nucl. Instrum. Methods Phys. Res., Sect. A **510**, 170 (2003).

[17] TESLA Technical Design Report, available at http://tesla.desy.de/new_pages/TDR_CD/PartV/fel.html, p. V-201.